New Generation of Carbon-Based Micro-Supercapacitors with High Specific Capacitance and Energy Densities

Abhi Gautham[1], Omar Nunez Cuacuas[1], Kevin Medici[1], Cedric Herrmann[1,2], Thilo Nordemann[1,2], Simon Schmidt[1,2], Asfaw Beyene[1], and Sam Kassegne[1†]

[1]Department of Mechanical Engineering, College of Engineering, San Diego State University, 5500 Campanile Drive, San Diego, CA, USA
[2]Universität der Bundeswehr München, Werner-Heisenberg-Weg 39, 85579 Neubiberg, Germany

Abstract

The demand for compact, high-performance energy-storage systems in microelectronics, mobile technologies, and implantable biomedical devices has accelerated interest in supercapacitors as high-power alternatives or complements to conventional batteries. Their rapid charge/discharge (CD) kinetics, long cycle lifetimes, and compatibility with microscale fabrication make them attractive for next-generation platforms; however, achieving high capacitance while maintaining efficient charge transport in small device footprints remains a critical challenge. In the meantime, carbon-based materials continue to dominate electrochemical double-layer capacitor development due to their high surface area, chemical stability, and favorable surface electrokinetics. In this study, we introduce a novel integrated, flexible carbon micro-supercapacitor technology. Electrochemical characterization demonstrates fast charge/discharge cycling (millisecond – seconds) and stable capacitive behavior. Further, the device exhibited area power density of 87.5 μW cm^{-2} and area energy density of 9.6 μWh cm^{-2} for a scan rate of 0.1 Vs, which is greater than the values reported for vertically aligned carbon nanotubes and multilayer reduced graphene oxide. These results establish carbon electrode platforms as a promising electrode material for high-performance supercapacitors, with strong potential for next-generation microelectronic and biomedical applications requiring ultrafast charging, high cycling stability, and long operational lifetimes.

Keywords: Supercapacitors, Energy storage, EDLC, Pseudo-capacitors, Carbon-based electrodes, Glassy Carbon, Graphene, Power density, Implantable medical devices.

†Address correspondences to Sam Kassegne • Professor of Mechanical Engineering, NanoFAB.SDSU Lab, Department of Mechanical Engineering, College of Engineering, San Diego State University, 5500 Campanile Drive, CA 92182-1323. E-mail: kassegne@sdsu.edu • Tel: (760) 402-7162.

1.Introduction

The growing demand for efficient, high-performance energy storage systems and the increasing proliferation of energy-intensive technologies, including mobile electronics, electric vehicles, and implantable biomedical devices, continues to motivate research into advanced energy storage solutions that offer alternatives to conventional batteries and capacitors [**1–3**]. In particular, implantable medical devices such as pacemakers and neuroprosthetics are required to operate reliably *in vivo* for extended periods, often exceeding five years, making frequent battery replacement impractical due to the need for surgical intervention. These constraints have driven growing interest in electrochemical supercapacitors, which offer fast charge/discharge (CD) cycles and long operational lifetimes [**4,5**]. Due to their large effective surface area and extremely thin dielectric layers, supercapacitors have emerged as a promising class of energy storage devices capable of storing significantly larger amounts of electric charge than electrolytic capacitors. These characteristics enable high capacitance and, consequently, large charge-storage capacity [**6**]. In addition to their high-power density, supercapacitors exhibit rapid charge/discharge (CD) capability, good energy density, and exceptional cycle life. As a result, they can be integrated with microelectronic systems either as stand-alone power sources or as complementary energy storage units alongside batteries, thereby expanding their range of applications. Recent research efforts have focused on improving both the energy and power densities of supercapacitors by optimizing electrode and electrolyte materials, device architectures, and fabrication methods [**5-6**].

As a background, supercapacitors store energy electrostatically, rather than chemically, enabling rapid charging/discharging (1–10 seconds), high power density, and a long lifespan of thousands of cycles. They are generally classified based on their charge storage mechanisms into electrochemical double-layer capacitors (EDLCs) and pseudo-capacitors. EDLCs store energy through electrostatic charge accumulation at the electrode–electrolyte interface and are therefore highly dependent on the accessible surface area of the electrode material. In contrast, pseudo-capacitors rely on fast, reversible faradaic redox reactions occurring at or near the electrode surface. Typical pseudocapacitive materials include transition metal oxides (e.g., RuO_2, MnO_2, Fe_3O_4) and conducting polymers, whereas EDLCs predominantly employ high-surface-area carbon-based materials.

In the meantime, carbon-based materials have gained widespread adoption in diverse applications, including sensors, microelectrodes, batteries, fuel cells, thin films, and neural interfaces, owing to their tunable mechanical, electrical, and electrochemical properties [**7–12**]. Among the various allotropes of carbon, graphene and glassy carbon (GC) stand out for their exceptional suitability in electrochemical energy storage applications. Graphene is widely regarded as the gold standard for electrical conductivity, while also exhibiting high mechanical strength and thermal conductivity [**13**]. Glassy carbon, on the other hand, is considered the gold standard for electrochemistry due to its chemical inertness, high electrochemical stability, purely capacitive charge injection behavior, and fast surface electrokinetics [**10-12**]. Importantly, both materials can be photolithographically patterned, enabling precise micro- and nanoscale device fabrication and broadening their applicability in miniaturized systems [**1,2,7,8**].

Building on this, here we introduce a micro-supercapacitor made of carbon (specifically glassy carbon) electrodes. This configuration offers several key advantages: (i) highly conductive carbon layers enabling rapid charge/discharge, (ii) GC layers with high charge-storage capacity (up to 61.5 mC cm^{-2} [**11**]) that enhance energy and power densities, (iii) tunable electrical and electrochemical properties, and (iv) mechanical robustness and flexibility. Moreover, the electrochemical performance of GC is highly tunable through controlled pyrolysis conditions, enabling optimization of its mechanical, electrical, and capacitive properties [**12**]. The intrinsic porosity of GC arising from closely spaced graphene ribbon domains effectively forms a network of nanoscale capacitors, which

contributes to its superior charge-storage behavior. This porosity, and hence the charge-storage capacity, can be further enhanced by adjusting synthesis parameters such as forming gas flow rates [**14-15**]. Together, these attributes have the potential to position the proposed system as a transformative approach for next-generation supercapacitors. In this context, the objective of this work is to develop a novel GC supercapacitor architecture that combines high charge-storage capacity with rapid CD capabilities. By leveraging the intrinsic advantages of carbon materials within a single, lithographically defined structure, this approach aims to address key limitations of existing supercapacitor technologies and enable compact, high-performance energy storage solutions suitable for implantable medical devices, mobile electronics, and other miniaturized systems.

2. Materials and Methods

2.1 Microfabrication

We introduce six distinct types of geometrical layouts with different numbers of electrode pairs and geometry. The designs are summarized in **Table 1** with one of them specifically designed to fit into a 0.5" diameter coin formfactor. The micro-supercapacitors introduced here were microfabricated using photolithography technology. Two platinum bump pads are located at either end of the device and alternating GC plates are electrically connected to one of the two bump pads. The microstructure includes first layer of GC plates, a base layer of polyimide (HD4100), metal interconnect traces, and a top insulation layer of HD4100.

As shown in **Figure 1,** the microfabrication started with SU-8 10 negative photoresist (MicroChem, USA) that was patterned on a silicon wafer with a ~0.5 µm silicon dioxide layer. After sequential solvent cleaning, dehydration baking, and oxygen plasma treatment to improve adhesion, SU-8 was spin-coated and soft-baked. The photoresist was then exposed to UV light through a dark-field mask, followed by post-exposure baking and development, to define the desired microstructures. These patterned SU-8 features were subsequently pyrolyzed in a N_2 atmosphere at 1000 °C, converting the polymer into conductive glassy carbon (GC) electrodes. To electrically insulate the GC electrodes while defining contact vias, a polyimide layer (HD-4100) was deposited and patterned. The substrate was then cleaned, followed by dehydration baking, plasma treatment, and spin coating of polyimide to achieve an approximately 6 µm thick film. After UV exposure, post-exposure baking, and development, electrical contact between GC electrodes and metal interconnects were formed. The polyimide was then cured under nitrogen. Metal interconnects were fabricated using a lift-off process, where a photoresist layer was patterned to define traces and contact pads, followed by sputter deposition of chromium and platinum. Subsequent lift-off in acetone removed unwanted metal, leaving well-defined electrodes, traces, and bump pads. A final polyimide insulation layer was applied to passivate the metal traces. In the final step, the devices were released from the silicon substrate by etching the underlying silicon dioxide layer using buffered hydrofluoric acid, yielding free-standing structures ready for electrochemical characterization.

2.2 Electrochemical Characterizations

Electrochemical characterization was performed using a conventional three-electrode cell configuration *in 0.01 M phosphate-buffered saline* (PBS, pH 7.4) to simulate physiological conditions. An Ag/AgCl electrode served as the reference, a platinum electrode as the counter, and individual microelectrodes as the working electrodes. Electrochemical impedance spectroscopy (EIS) was employed as a non-destructive technique to study charge transport at the electrode-electrolyte interface over a frequency range of 10 Hz to 10 kHz using a small sinusoidal input signal. The impedance response was interpreted using an equivalent circuit model consisting of solution resistance, double-layer capacitance (modeled as a constant phase element for carbon electrodes),

charge-transfer resistance, and Warburg impedance. Bode and Nyquist plots were analyzed to extract information on solution resistance, capacitive behavior, charge-transfer processes, and diffusion-limited effects.

Cyclic voltammetry (CV) was used to evaluate charge-storage capacity (CSC) and surface electrochemical behavior by sweeping the electrode potential within the material's water window. CSC was calculated from the cathodic current integral and distinguished from charge-injection capacity (CIC), which represents the safely injectable charge. Redox characterization was conducted using potassium ferrocyanide as a benchmark redox couple to assess reaction reversibility, electron-transfer kinetics, and diffusion behavior through peak separation and scan-rate dependence. Voltage transient analysis was further employed to determine CIC by applying controlled current pulses and ensuring electrode polarization remained within safe potential limits. Finally, galvanostatic charge–discharge testing was used to evaluate electrochemical capacitance, charge–discharge behavior, cyclability, energy density, and power density.

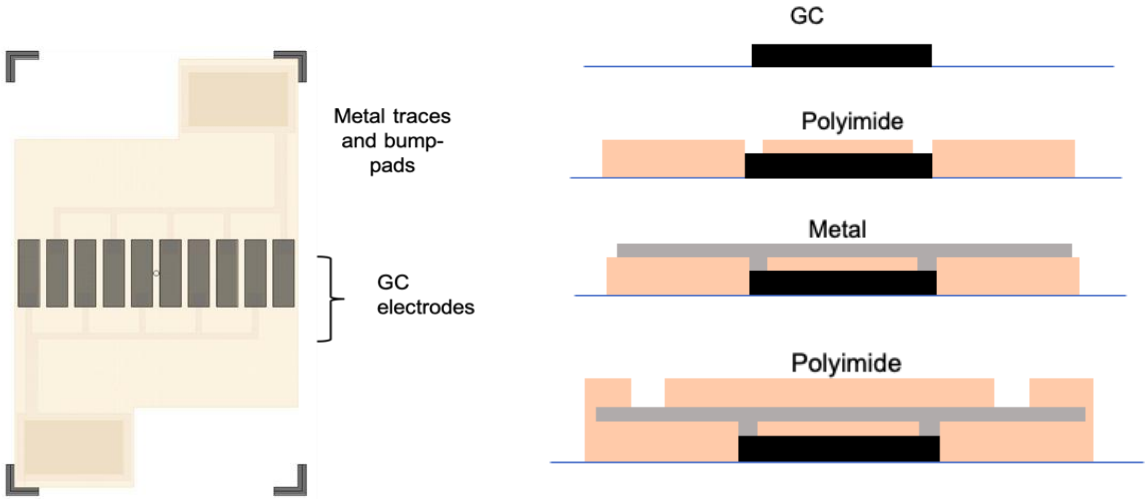

Figure 1: Microfabrication steps for the supercapacitors with GC electrodes and metal bump-pads. The electrodes are made of GC with a base insulation of polyimide, traces of platinum (with chromium adhesion layer), and top insulation of polyimide.

Table 1: Geometrical details of the four micro-supercapacitors considered in this study.

Design Type	Electrode Geometry (all in μm)				# Electrode Pairs
	L	W	Spacing	Thickness	
D1	2500	750	250	15	**10**
D2	2500	400	50	15	**20**
D3	2000	50	100	15	**12**
D4	2000	250	250	15	**48**
		100	100	15	**52**
D5	Varying	500	200	15	**12**
D6	Varying (4000)	300	100	15	**24**

3. Results

3.1 Electrochemical Characterization Results

The devices that were fabricated are shown in **Figure 2.** This section presents the detailed electrochemical characterization outcomes for these devices. These include EIS, CV, voltage transient analysis, and galvanostatic charge/discharge experiments. EIS was performed for all design configurations under identical electrochemical conditions, as described earlier. Further, this section provides a comparative analysis as well as physical interpretation and significance of results amongst the designs considered. It also summarizes the Nyquist and Bode plot results obtained for each configuration.

Figure 3 presents a summary of the CV and EIS outcomes for each of the six devices considered in this study. **Table 3** summarizes the electrical and electrochemical characterizations of the supercapacitors. For example, for design D1, a mean impedance of 32.47 ± 11.2 kΩ was measured at 1 kHz, while the phase-versus-frequency plot exhibits characteristic capacitive behavior. As shown in **Figure 4**, CV was also carried out in $Fe(CN_6)^{3-/4-}$ solution. The CV data obtained at different scan rates and the peak currents for both anodic and cathodic processes were plotted as a function of scan rate. Following data fitting, a linear relationship was observed between the anodic and cathodic peak currents and the square root of the scan rate, consistent with the Randles–Ševčík equation. This behavior indicates diffusion-controlled surface kinetics. In addition, for an electrochemically reversible process, the separation between anodic and cathodic peak potential is approximately 57 mV at 25 °C for design D3, for example.

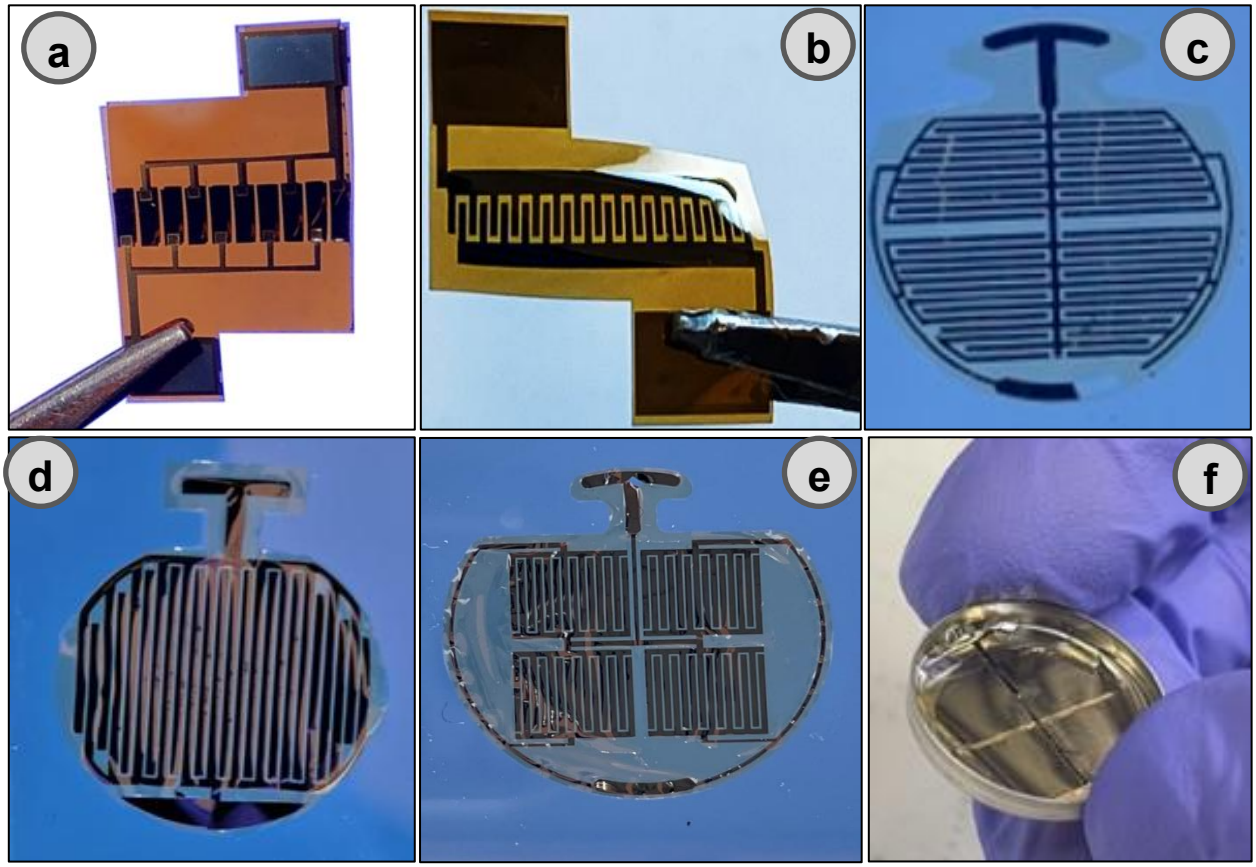

Figure 2: The microfabricated supercapacitors (a) D1, (b) D2, (c) D3, (d) D4. (e) D5, and (f) D6

Table 2: Summary of electrochemical characterization of the four micro-supercapacitors considered in this study. t_c = time for charging, t_f = time for discharging.

Design Type	Q (stored charge)	|Z| at 1KHz	C/D (Charge/Discharge)		
			V_f (Volts)	t_C (sec)	t_D (sec)
D1	**140 mC/cm^2**	**15.4 kΩ**	0.4V, 1.0V, 0.0V	3 secs	2 secs
D2	**40 mC/cm^2**	**22.65 kΩ**	0.2V, 0.22V	20 secs	7.5 secs
D3	**NA**	**7.5 kΩ**	**NA**	**NA**	**NA**
D4	**140 mC/cm^2**	**1.1 kΩ**	0.2V, 0.22V, 0.05V	3 secs	3 secs
	28 mC/cm^2	**4.5 kΩ**			
D5	**22 mC/cm^2**	**9 kΩ, 30 kΩ**	0.5V, 0.6V, 0.23V	3 secs	3 secs
D6	**25 mC/cm^2**	**25 kΩ**	0.5V, 0.8V, 0.3V	3 secs	3 secs

Voltage transient responses were also recorded for the devices in response to four different current waveforms, each evaluated at three current amplitudes: 100 μA, 250 μA, and 500 μA. **Figure 5** shows the resulting voltage transients obtained by applying single current pulses of the various waveforms, showing mean responses for *n = 5* devices in each case. Further analysis of the voltage transient response data was performed to enable comparison across several physical parameters. The parameter V_a is defined as the near-instantaneous voltage change occurring either at the onset of the current pulse or immediately following pulse termination. This parameter reflects the contribution of ohmic electrolyte/solution resistance and overpotential effects [**7**].

In this study, V_a was measured approximately 20 μs after pulse termination, corresponding to the time at which the current effectively decays to zero. The parameters E_{ma} and E_{mc} represent the maximum anodic and cathodic polarization at the electrode–electrolyte interface, respectively. $V_{max,neg}$ is the maximum voltage attained in response to cathodic current pulse while $V_{max,pos}$ signifies the maximum voltage attained in response to anodic current pulse. V_u signifies the unrecovered voltage, i.e. amount of voltage residual in the system after termination of the input current pulse. The energy, E_{load}, represents the energy consumed in the electrode and the solution during the stimulation of current pulse.

3.2 Galvanostatic Charge/Discharge results

Galvanostatic charge discharge experiment was carried out for the supercapacitor to access performance parameters such as charge/discharge behavior, specific capacitance, energy and power densities. **Figure 6** demonstrates the charge and discharge curves for the various supercapacitor devices under different input currents. For example, the charging process is shown in blue, and the discharging process in orange. A time of 6 seconds was considered. The supercapacitors absorbed almost the maximum charge within 1 second and subsequently released it within 1-3 seconds. The potential value never reached 0, always settling closer to a certain value.

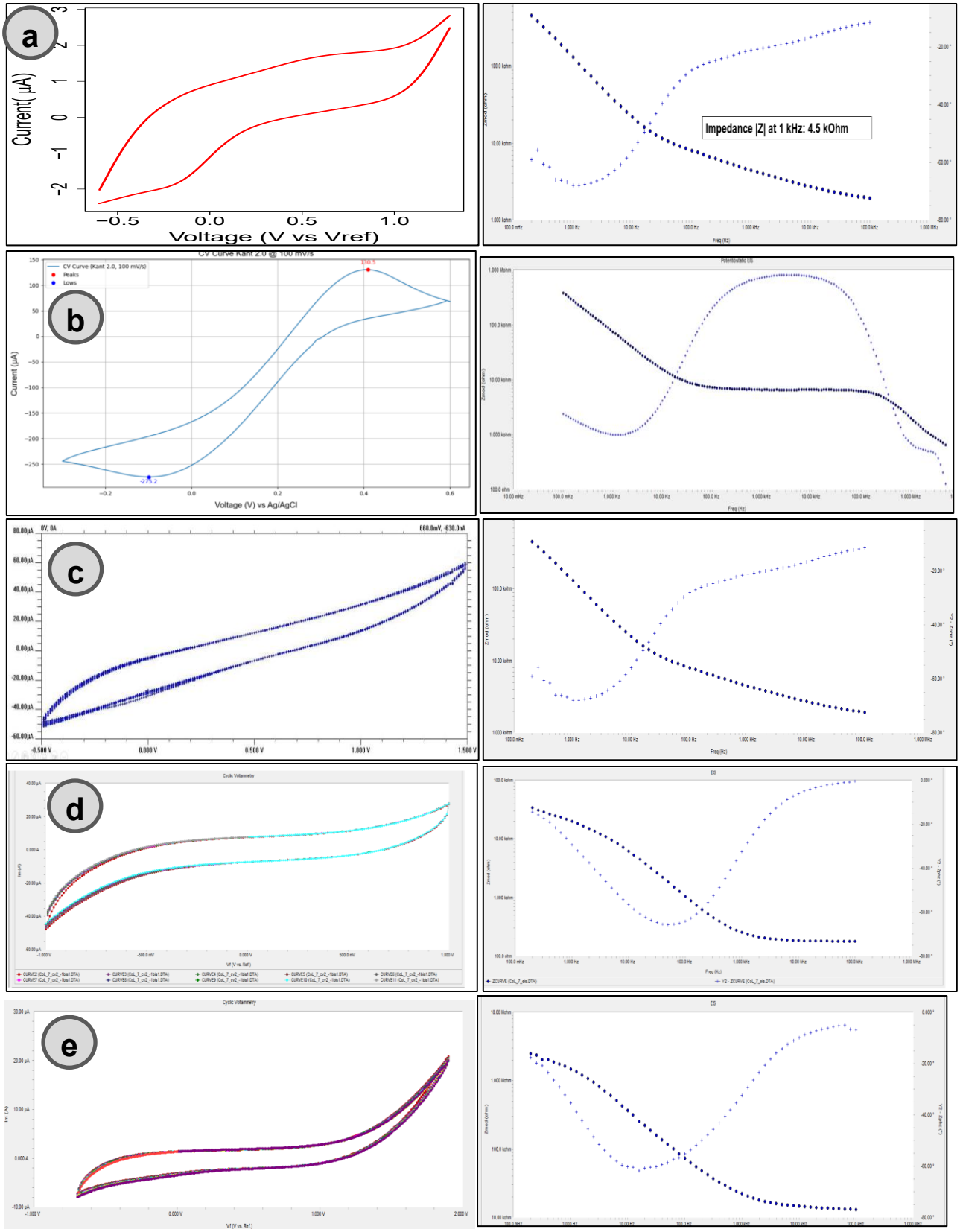

Figure 3: Cyclic voltammetry and Bode plots of EIS characterizations of the supercapacitors in PBS solution (a) D1, (b) D3, (c) D4, (d) D5, and (e) D6. For example, for D1: |Z| = 32.47 ± 11.2 kΩ at 1kHz. Charge Storage Capacity: 140 μC/cm^2.

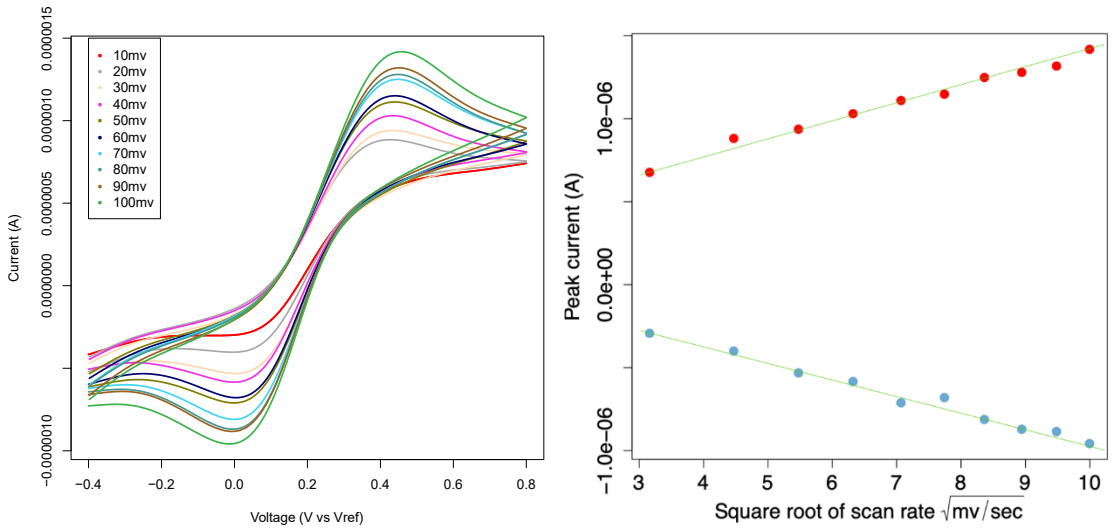

Figure 4: (a) Cyclic Voltammetry for D2 supercapacitor using $Fe(CN_6)^{3-/4-}$ solution (b) cathodic and anodic peak current vs scan rate data, in accordance with Randel-Sevcik equation.

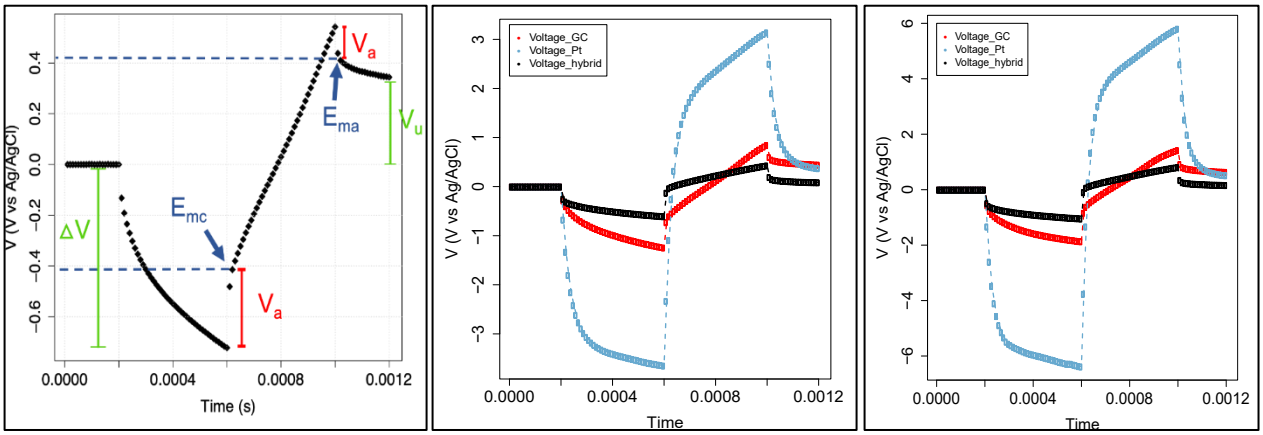

Figure 5: Voltage transient analysis results for (i) biphasic balanced input current pulse of different amplitudes - (ii) 100uA (iii) 250uA (iv) 500uA (n=5 for each case).

4. Discussions

4.1 Charge Storage Mechanism and Electrochemical Behavior

Electrochemical characterization confirms that the proposed glassy carbon (GC) micro-supercapacitors operate predominantly through electrochemical double-layer capacitance (EDLC). The approximately rectangular cyclic voltammetry (CV) profiles observed within the water window indicate ideal capacitive behavior with minimal faradaic contribution. The absence of pronounced redox peaks supports the conclusion that charge storage is dominated by electrostatic ion accumulation at the electrode–electrolyte interface rather than surface redox reactions. The diffusion-controlled kinetics observed in the ferrocyanide redox experiments further confirm that the electrode–electrolyte interface remains electrochemically active and reversible. The linear relationship between peak current and the square root of scan rate is consistent with well-established electrochemical theory and indicates efficient mass transport at the GC surface. Together, these results demonstrate that the lithographically defined glassy carbon architecture maintains stable and reversible electrochemical characteristics.

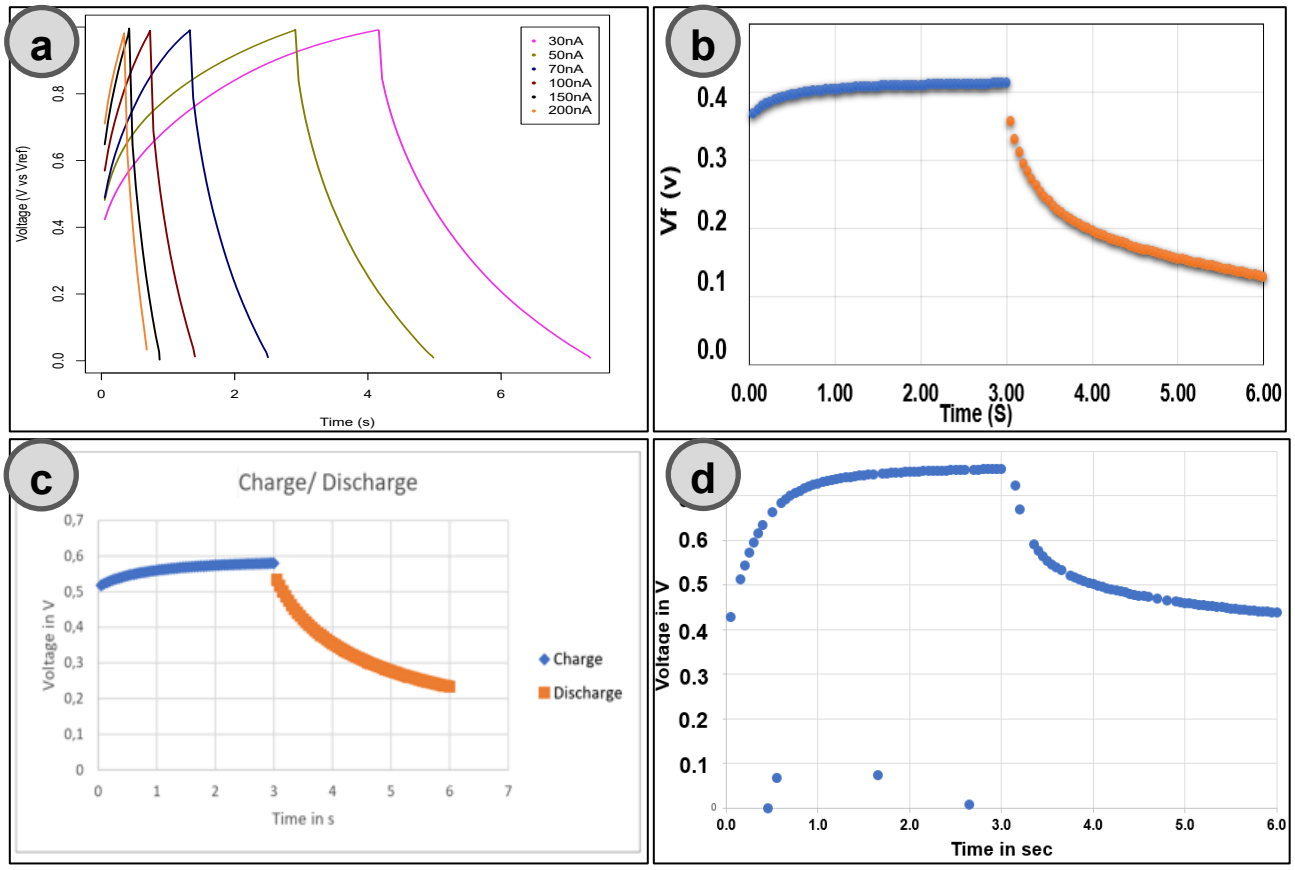

Figure 6: Charge and discharge (C/D) voltage vs time curve for four of the six supercapacitors (a) D1, (b) D4, (c) D5, and (d) D6.

4.2 Impedance and Charge Transport Characteristics

Electrochemical impedance spectroscopy (EIS) revealed relatively low impedance values at 1 kHz and a phase response characteristic of capacitive systems. The small high-frequency intercept in the Nyquist plot corresponds to solution resistance, while the near-vertical low-frequency region reflects dominant double-layer behavior. The low internal resistance is particularly significant for microscale energy storage applications, where compact geometries can otherwise introduce significant series resistance. The use of platinum interconnects combined with conductive glassy carbon plates contributes to efficient electron transport, while the accessible electrode surface area supports rapid ion migration within the electrolyte. The modest variability in impedance across device geometries likely arises from differences in electrode spacing, plate thickness, and effective surface area. Designs with smaller spacing are expected to reduce ion diffusion path lengths, thereby lowering internal resistance and improving high-rate performance.

4.3 Galvanostatic Charge–Discharge Performance

Galvanostatic charge/discharge (C/D) measurements demonstrate rapid charging and discharging behavior, with near-linear voltage–time profiles indicative of capacitive operation. The short charge times (on the order of seconds) confirm the high-power capability of the GC micro-supercapacitors. The observed deviation from perfectly symmetric charge–discharge slopes at higher current amplitudes can be attributed to internal resistance and ion transport limitations. As current increases, voltage drops due to equivalent series resistance (ESR) becomes more pronounced, slightly

reducing energy efficiency. The device-to-device variability observed in capacitance values likely reflects fabrication-induced variations in GC microstructure, such as porosity and surface roughness, both of which influence effective electrochemical surface area. Additionally, small inconsistencies in pyrolysis conditions can alter the ratio of sp^2 to sp^3 bonding in glassy carbon, thereby affecting conductivity and charge storage. Despite this variability, the overall performance trends are consistent across geometries and current densities, demonstrating reproducible capacitive behavior.

4.4 Influence of Glassy Carbon Microstructure

The electrochemical performance of glassy carbon electrodes is intrinsically linked to their microstructure. Glassy carbon consists of interconnected graphene-like domains embedded in an amorphous carbon matrix. This hybrid structure provides high electrical conductivity via sp^2-hybridized networks, mechanical robustness due to sp^3 crosslinking, and intrinsic nanoscale porosity that enhances accessible surface area. The pyrolysis-driven formation of GC introduces nanoscale voids and ribbon-like carbon domains, which effectively increase the electrochemically active area relative to the geometric footprint. This structural characteristic explains the observed charge-storage capacity and supports the EDLC mechanism. Optimization of pyrolysis parameters including heating rate, dwell time, and gas composition offers a pathway for further performance enhancement. Increased porosity could raise capacitance but must be balanced against mechanical integrity and electrical conductivity.

4.5 Comparison with Carbon-Based Supercapacitors

Carbon-based micro-supercapacitors reported in literature frequently rely on vertically aligned carbon nanotubes, reduced graphene oxide, or activated carbon films. While these materials can achieve high gravimetric capacitance, they often face challenges related to integration, mechanical stability, or scalable microfabrication.

In contrast, the glassy carbon architecture presented here offers several advantages such as compatibility with standard photolithographic processes, structural robustness suitable for flexible or implantable systems, stable electrochemical behavior without significant degradation, and rapid charge/discharge capability within compact footprints. Although the areal capacitance values are lower than those reported for some nanostructured graphene-based systems, the present approach emphasizes manufacturability, mechanical stability, and integration readiness rather than purely maximizing gravimetric metrics.

4.6 Implications for Miniaturized and Biomedical Systems

For implantable and flexible electronics, reliability and stability are often more critical than absolute energy density. The stable capacitive response, rapid charge/discharge behavior, and low impedance demonstrated here make GC micro-supercapacitors promising candidates for power buffering in implantable neurostimulators, hybrid battery–supercapacitor energy management systems, energy harvesting storage modules, and compact wearable electronics. The use of phosphate-buffered saline as the test electrolyte further supports the relevance of this platform for physiological environments.

4.7 Limitations and Future Directions

While the present study demonstrates promising performance, several areas warrant further investigation such as long-term cycling stability and capacitance retention, optimization of electrode geometry for improved energy density, reduction of device-to-device variability, exploration of gel or solid-state electrolytes for full device integration, and volumetric normalization of capacitance for direct comparison to literature. Future work should also investigate hybrid architectures incorporating pseudocapacitive coatings to enhance energy density while maintaining rapid charge–discharge kinetics.

5. Conclusions

In this work, we developed and evaluated a lithographically defined glassy carbon (GC) micro-supercapacitor architecture designed for compact, high-performance energy storage applications. The integrated device combines pyrolyzed glassy carbon electrodes, metallic interconnects, and polyimide insulation layers within a flexible microscale platform compatible with standard microfabrication processes.

Electrochemical impedance spectroscopy confirmed low internal resistance and predominantly capacitive behavior, while cyclic voltammetry exhibited near-rectangular profiles characteristic of electrochemical double-layer capacitance (EDLC). Galvanostatic charge–discharge measurements demonstrated rapid charge and discharge kinetics with stable capacitive performance across multiple current densities. The observed charge-storage capacity and power characteristics highlight the ability of glassy carbon to provide efficient ion accumulation and fast electron transport within a compact footprint.

The results indicate that charge storage in the present architecture is governed primarily by double-layer mechanisms, supported by the intrinsic nanoscale porosity and mixed sp^2/sp^3 bonding structure of glassy carbon. Although device-to-device variability was observed, performance trends remained consistent across geometrical configurations, demonstrating reproducible capacitive behavior. Compared to many nanostructured carbon systems that prioritize gravimetric capacitance, the proposed GC micro-supercapacitor emphasizes structural robustness, lithographic scalability, and integration readiness. These attributes make it particularly attractive for miniaturized and implantable systems requiring rapid charge–discharge capability, long-term stability, and compatibility with flexible substrates.

Future work will focus on reducing variability, optimizing electrode geometry and pyrolysis parameters, evaluating long-term cycling stability, and exploring solid-state electrolytes to enable fully integrated micro-energy storage modules. Overall, this study establishes glassy carbon as a viable and scalable electrode platform for next-generation micro-supercapacitors and highlights its potential for compact, high-power energy storage in biomedical and microelectronic applications.

Acknowledgment
This material is based on research work supported by the **Center for Neurotechnology** (CNT), a National Science Foundation Engineering Research Center (EEC-1028725) and **NSF AccelNet**: Broadening Carbon Ring program (Award Number: 2301898).

Competing Financial Interests
The authors declare no competing financial interests.

Data Availability Statement
Data is available on request.

Author contributions:
AB, ONC, KM, CH, TN, and **SS** fabricated the micro-supercapacitors and carried out the electrochemical characterizations for each of the devices. **AB** edited the manuscript and wrote the introduction and conclusion section of the paper. **SK** formulated the concept, supervised the project, structured the outline of the paper, edited the manuscript, and wrote the introduction, discussion and conclusion section of the paper.

References

1. MacKenzie, J. D. & Ho, C. "*Perspectives on energy storage for flexible electronic systems*," Proc. IEEE 103, 535–553 (2015).
2. Gwon, H. et al. "*Recent progress on flexible lithium rechargeable batteries*," Energy Environ. Sci. 7, 538–551 (2014).
3. Miller, J. R. & Simon, P. "*Electrochemical Capacitors for Energy Management*," Science 321, 651-652 (2008).
4. Simon, P. & Gogotsi, Y. "*Materials for electrochemical capacitors*," Nat. Mater. 7, 845-854 (2008).
5. Beidaghi, M., Y.J.E. Gogotsi, and E. Science, *Capacitive energy storage in micro-scale devices: recent advances in design and fabrication of micro-supercapacitors.* 2014. **7**(3): p. 867-884.
6. Yang, J. and S.J.C. Gunasekaran, *Electrochemically reduced graphene oxide sheets for use in high performance supercapacitors.* 2013. 51: p. 36-44.
7. Yu, A., Roes, I., Davies, A., Chena, Z., "*Ultrathin, transparent, and flexible graphene films for supercapacitor application*", Appl. Phys. Lett. 96, 253105 (2010)
8. O. J. A. Schueller, S. T. Brittain, C. Marzolin, and G. M. Whitesides. *Fabrication and Characterization of Glassy Carbon MEMS*. *Chem. Mate*r. 9, 1399–1406 (1997).
9. S. Ranganathan, R.L. McCreery, S.M. Majji, M. Madou, J. *Photoresist-Derived Carbon for Microelectromechanical Systems and Electrochemical Applications*. *Electrochem. Soc.* 147:277-282, (20000.
10. Vomero, M, van Niekerk, P, Kassegne, S., *et al,* "*Novel Pattern Transfer Technique for Mounting Glassy Carbon Microelectrodes on Polymeric Flexible Substrates*", JMM (Journal of Micromechanics and Microengineering), Volume 26, Number 2, 2016.
11. Vomero M., Castagnola E., Ciarpella F., Maggiolini E., Goshi N., Zucchini E., Carli S., Fadiga L., Kassegne S., Ricci D. *Highly Stable Glassy Carbon Interfaces for Long-Term Neural Stimulation and Low-Noise Recording of Brain Activity*. *Nature Sci. Rep* 7 (2017).
12. Kassegne, S., Vomero, M., Gavuglio, R., Hirabayashi, M., Özyilmaz, E., Nguyen, S., Rodriguez, J., Özyilmaz, E., van Niekerk, P., Khosla, A., "*Electrical Impedance, Electrochemistry, Mechanical Stiffness, and Hardness Tunability in Glassy Carbon MEMS* μ*ECoG Electrodes*", J. of Microelectronics Engineering, Volume 133, Pages 36–44, 2015.
13. Novoselov, K.S., et al. *Science,* 306:666–669 (2004).
14. Sharma, S., Kamath, R., Madou, M. "*Porous Glassy Carbon Formed by Rapid Pyrolysis of Phenol-Formaldehyde Resins and its Performance as Electrode Material for Electrochemical Double Layer Capacitors*", *J. Analytical and Applied Pyrolysis* 108:12-18 (2014).
15. Mardegan, A., Kamath, R., Sharma, S., Scopece, P., Ugo, P., Madou, M. "*Optimization of carbon electrodes derived from epoxy-based photoresist", J. Electrochemical Society* 160(8):B132-B137 (2013).
16. Meng, C., O.Z. Gall, and P.P.J.B.m. Irazoqui, "*A flexible super-capacitive solid-state power supply for miniature implantable medical devices",* 2013. 15(6): p. 973-983.
17. Chen, H., B. Wei, and D.J.I.T.o.P.E. Ma, "*Energy storage and management system with carbon nanotube supercapacitor and multidirectional power delivery capability for autonomous wireless sensor nodes",* 2010. 25(12): p. 2897-2909.
18. Simjee, F. and P.H. Chou. "*Everlast: long-life, supercapacitor-operated wireless sensor node*", in *Proceedings of the 2006 international symposium on Low power electronics and design*. 2006. ACM.
19. Simjee, F.I. and P.H.J.I.T.o.p.e. Chou, "*Efficient charging of supercapacitors for extended lifetime of wireless sensor nodes",* 2008. 23(3): p. 1526-1536.
20. Simon, P. and Y. Gogotsi, "*Materials for electrochemical capacitors*, in *Nanoscience And Technology: A Collection of Reviews from Nature Journals*", 2010, World Scientific. p. 320-329.
21. Chen, S.-M., et al., "*Recent advancements in electrode materials for the high-performance electrochemical supercapacitors: a revie,".* 2014. 9(8): p. 4072-4085.
22. Zhang, L.L. and X.J.C.S.R. Zhao, "*Carbon-based materials as supercapacitor electrodes",* 2009. 38(9): p. 2520-2531.

23. Huang, X., et al., *Electric double layer capacitors using activated carbon prepared from pyrolytic treatment of sugar as their electrodes.* 2003. 135: p. 235-236.
24. Hsia, B.; Marschewski, J.; Wang, S.; In, J. Bn; Carraro, C.; Poulikakos, D.; Grigoropoulos, C. P.; Maboudian, R. "*Highly Flexible, All Solid-State MicroSupercapacitors from Vertically Aligned Carbon Nanotubes"*. Nanotechnology 2014, 25 (5), 55401.
25. J. J. Yoo, K. Balakrishnan, J. Huang, V. Meunier, B. G. Sumpter, A. Srivastava, M. Conway, A. L. Mohana Reddy, J. Yu, R. Vajtai, P. M. Ajayan, Nano Lett. 2011, 11, 1423.